International Journal of Fluid Power 1 (2000) No. 2 pp. 11-27

DERIVATION OF DESIGN REQUIREMENTS FOR OPTIMIZATION OF A HIGH PERFORMANCE HYDROSTATIC ACTUATION SYSTEM

Saeid R. Habibi and Gurwinder Singh

Department of Mechanical Engineering, University of Saskatchewan, 57 Campus Drive, Saskatoon, Saskatchewan, Canada S7N 5A9
saeid_habibi@engr.usask.ca

Abstract

The competitive global market dictates greater quality of product models produced at lower cost and in shorter duration. During the past two decades, the efficiency of production processes and the quality of products have been differentiating factors in establishing competitive advantage in mature industries such as fluid power. The survival of such industries is increasingly dependent on their ability of optimizing their component characteristics as well as integrating these in complex subsystems. Reduction of cost of poor quality is thus critical. This cost often originates from inadequate or sub-optimal design requirements. Mature industries involved in the design and production of complex systems, have recognized the importance of design requirements definition in reducing cost and increasing profitability.

This paper considers linking of system requirements to design parameters for a high performance actuation system referred to as the Electro Hydraulic Actuator (EHA). EHA is based on the hydrostatic actuation concept. It has been prototyped and has demonstrated a very high level of performance. The mathematical model of EHA is reviewed and used for linking its performance to its design parameters through a set of mathematical functions. The actual and expected performances of the prototype are compared in order to validate the proposed mathematical functions and an improved design is proposed.

Keywords: hydrostatic, electro-hydraulic actuation, robotics

1 Introduction to EHA

EHA uses hydrostatic transmission that is used to allow a variable transmission of power by connecting a pump directly to a hydraulic actuator, Watton (1989), Korn (1972), Manring et al (1998), Anderson et al (1998). Most hydrostatic circuits use a constant speed piston pump with variable displacement. The movement of the hydraulic actuator is regulated by moving a swash plate on the pump that changes the magnitude and direction of flow, Watton (1989). These circuits are energy inefficient, as the pump continuously runs irrespective of the motion of the actuator. Furthermore, use of variable displacement (piston) pumps can result in ripple effects that could degrade high precision motion, Watton (1989). An alternative strategy is to vary the flow by changing the speed and direction of a fixed displacement pump, Watton (1989), Korn (1972), Arnautovic (1993). This strategy could result in smaller ripples at medium to high flow-rates. However, the commercial progress of such hydrostatic actuation has been affected by the presence of a dead-band (Fig. 1) with an effect similar to backlash, thus limiting the positional accuracy and stability of this type of system. This deficiency is alleviated in the EHA concept through a high gain cascaded flow control strategy proposed in Habibi and Goldenberg (1999a).

A proposed design for a high performance EHA and details of its assembly configurations are specified in

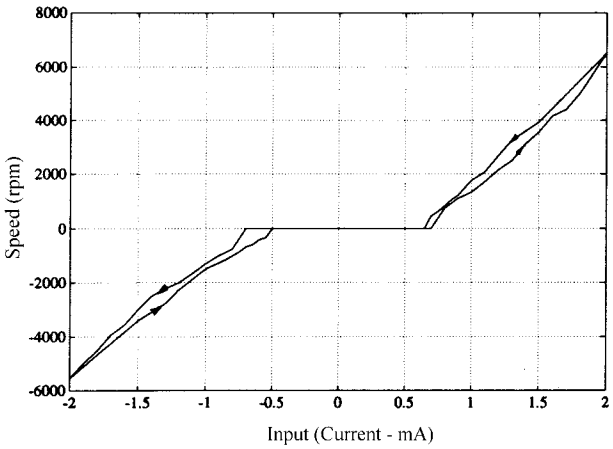

Fig. 1: *Deadband, Arnautovic (1993)*

This manuscript was received on 12 January 2000 and was accepted after revision for publication on 6 July 2000

sections 2 and 3. A new symmetrical linear actuator specifically designed for EHA is described in section 4. Section 5 proposes a linearized mathematical model. Categorization of design parameters and their link to EHA's performance are discussed in section 6. A prototype of EHA is described and analyzed in section 7. The design of the EHA prototype is optimized in section 8. Section 9 contains the concluding remarks.

2 Design of EHA

A high performance ElectroHydraulic Actuator (EHA) has been prototyped and consists of: (i) a variable speed, electrically driven gear pump, (ii) a symmetrical actuator (a rotary actuator or a linear actuator specifically developed for EHA), (iii) pressure and position sensors, (iv) accumulator, (v) pressure relief safety sub-circuit, and (vi) filtering sub-circuits. Item (v) can be implemented through careful pump design and electronic sensing thus reducing the overall weight of the system. Item (vi) is introduced subject only to reliability requirements.

In this system, the pressure difference across the actuator (labeled symmetrical actuator in Fig. 2) is a consequence of pumping action (pump flow) and, results in exertion of force and movement of the external load. In the EHA prototype, a bi-directional gear pump is used. The internal seals of the pump are modified to withstand a maximum case pressure of 690 kPa (100 psi). This allows the attachment of the pump's case drain to EHA's accumulator that is maintained at 310 kPa (45 psi). This connection is made via a check valve of 7 kPa (1 psi) break pressure.

This type of hydrostatic actuation is susceptible to the presence of a dead-band that is largely due to a nonlinear friction effect (including static and coulomb friction) at the pump motor interface with an effect similar to backlash, as shown in Fig. 1, thus limiting its positional accuracy and stability, Arnautovic (1993), Doeblin (1972). A prototype of EHA has been produced in which the dead-band is alleviated through appropriate component selection and the implementation of a high gain inner-loop control strategy involving pump speed (flow) feedback. Subsequently, EHA is capable of a high level of performance as demonstrated by the prototype. The performance data of its prototype are as follows:

Maximum working pressure	20700 kPa (3000 psi)
Maximum output force	10.5 kN
Maximum piston stroke	12 cm
Closed loop position accuracy	0.01 mm (limited by encoder accuracy)
Force to weight ratio	1.1 kN/kg (actuator)
Deadband	Negligible
Rise time	0.3 sec (load of 20 kg)
Settling time	0.5 sec (load of 20 kg)

3 Configurations

EHA may be configured in a similar way to conventional hydraulic systems, where the (power) supply is detached from the actuator in order to increase the force to mass ratio at the actuation point. The supply module (Fig. 2) may be detached from the actuation module (Fig. 2) and linked to it by using flexible hosing. Like other hydraulic systems, the actuation module could be designed to provide linear, rotary or continuous rotational motion. This concept is particularly appealing for robotic systems, where the force to mass

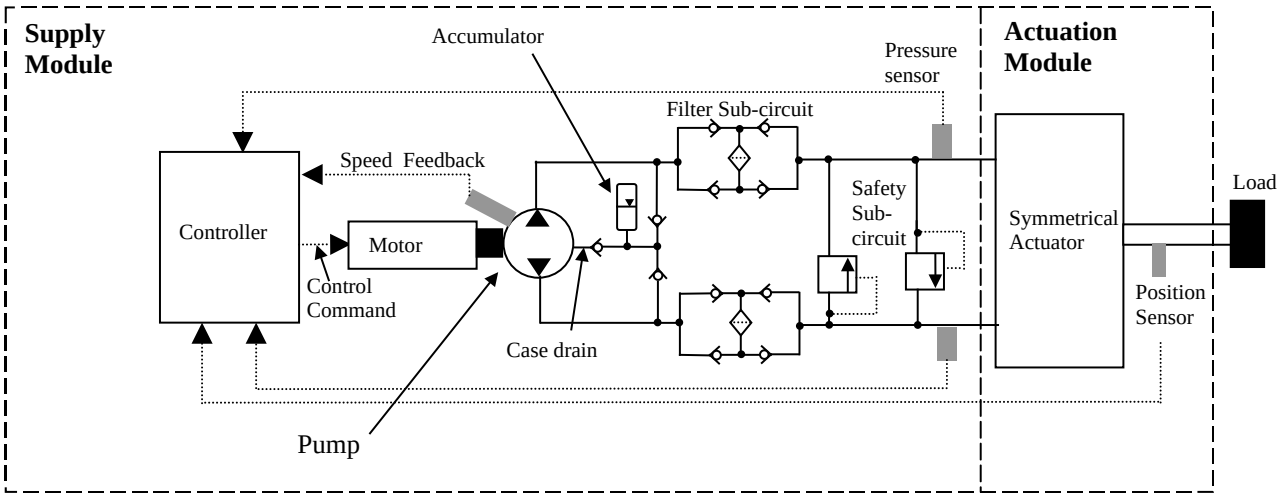

Fig. 2: *EHA circuit diagram*

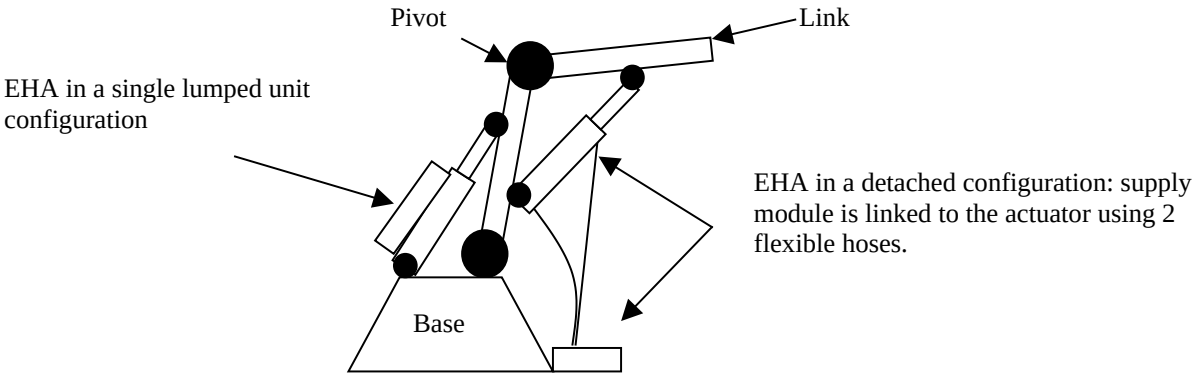

Fig. 3: *Two link robot with the two configurations of EHA*

ratio of the actuation system plays a very significant role in the bulk and overall mass of a manipulator (heavy actuation units would require heavier links, thus compounding the difficulty of minimizing the overall mass of the robot – this is particularly evident in robots with high degrees of freedom). The disadvantage of separating the supply module from the actuation module is a resulting reduction in the hydraulic stiffness. Alternatively, EHA can be made up of one single piece with the supply module being an integral part of the actuation module (Fig. 2). A simple example of a 2 degrees of freedom robot using both configurations of EHA with linear actuation is shown in Fig. 3.

4 Symmetrical Actuator

EHA requires a symmetrical actuator in order to ensure flow balance between the actuator and the pump. A symmetrical linear actuator is specifically designed for this type of systems. In this design, there are two working chambers C1 and C2 as illustrated in Fig. 4. The solid rod of the conventional piston is replaced by a hollow cylinder that is closed at one end and has a circular disc around the opening at the other end. The surface area of the closed end of the cylinder, A1, is made equal to the area A2 of the disc. A1 and A2 are the active areas of the two pressure chambers and are therefore made equal (A1 = A2 = A). Chamber C3 can be opened to the atmosphere or could be filled with pressurized gas or fluid in applications, where a bias is required to counter balance a dead weight acting under gravity. The contact between the cylinder and the fixed body of the actuator is through low friction seals. Hydraulic fluid enters the two chambers of the actuator through openings O1 and O2.

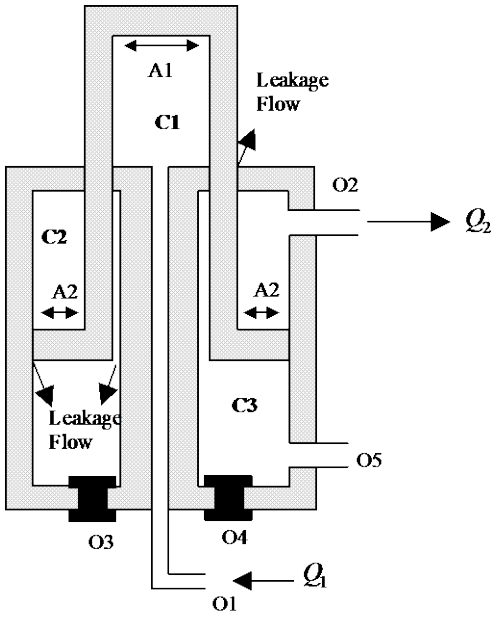

Fig. 4: *Linear actuator*

It is recognized that there will be some external leakage across the seal into chamber C3. The openings O3 and O4 allow draining of fluid from this chamber. Opening O5 is provided to allow pressurization of chamber C3 for specialized applications. This design has a number of advantages which meet the requirements of hydrostatic circuits such that in each direction of stroke:

- maximum saturation speed and torque are the same,
- the dynamic characteristic is the same, thus simplifying the controller structure, and
- the quantities of fluid displaced by the two primary chambers of the actuator are equal.

These requirements are not satisfied by conventional single rod pistons. The dynamic significance of this design is considered in detail in Habibi and Goldenberg (1999b).

5 Mathematical Model

A mathematical model of EHA and its components is described in Habibi and Goldenberg (1999c). A review of this model is presented in this section. The model is linearized and used for the generation of equations relating design parameters to performance.

5.1 Controller Structure

The control strategy used is critical to the performance of EHA. Here, two control loops are used as shown in Fig. 5. The effect of the dead-band in hydrostatic circuits (Fig. 1) is removed through an

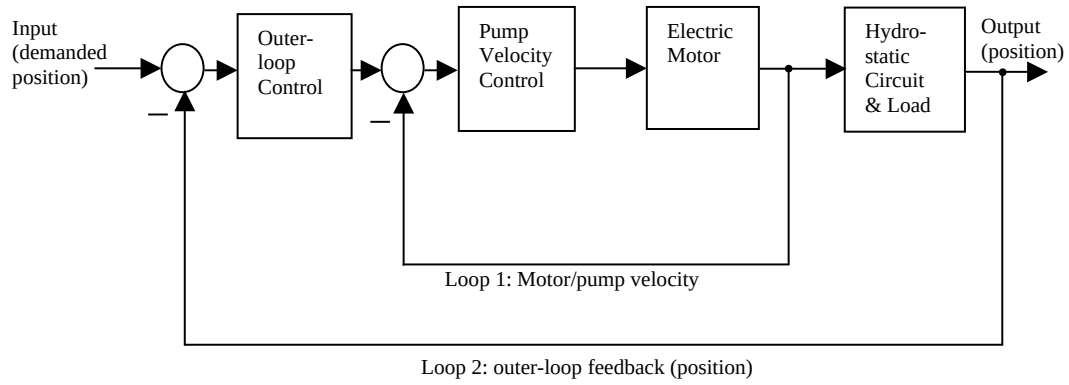

Fig. 5: *Control block diagram*

inner-loop high-gain controller (loop 1), which would regulate the speed of pumping (flow) and desensitize this system to dead-band (this can be confirmed through sensitivity analysis as shown in the following section). The outer-loop controller (loop 2) allows precision control of the output variable, which could be speed and/or position, Habibi and Goldenberg et al (1999a).

5.2 Electrical Motor/Pump Sub-system

The hydraulic pump is driven by an AC electrical motor. The equivalent mathematical model of such electrical motors is well established and a simplified model is used as derived in Del Toro (1990) and Van de Vegte (1994). In this case, the electrical part of the motor can be described by a first order transfer function such that: $I_c = G_1 V_c$ and,

$$G_1 = \frac{1/R_c}{L_c/R_c s + 1} = \frac{K_e}{\tau_e s + 1} \tag{1}$$

where τ_e and K_e are the motor's electrical circuit time constant and gain.

The torque generated by the motor is characterized by $T_m = K_c I_c - K_\omega \dot{\theta}$. Given that the motor is connected directly to the pump, the torque exerted on the pump is given by, Watton (1989):

$$T_m = J_{pm}\dot{\omega}_p + K_{p_{visc}}\omega_p + T_{DB} + D_p(P_a - P_b) \tag{2}$$

Rearranging the above equations, the speed of the pump is obtained as:

$$\omega_p = G_2 K_c I_c - G_2 D_p (P_a - P_b) - G_2 T_{DB} \tag{3}$$

where, from Eq. 2, the transfer function of the mechanical part of the motor is approximated by G_2 such that:

$$G_2 = \frac{1/(K_{p_{visc}} + K_\omega)}{\frac{J_{pm}}{(K_{p_{visc}} + K_\omega)}s + 1} = \frac{K_m}{\tau_m s + 1} \tag{4}$$

T_{DB} denotes nonlinear friction (including static and coulomb friction) at the pump motor interface that causes the effect shown in Fig. 1. The effect of T_{DB} can be minimized by using an inner-loop high-gain motor velocity-feedback as shown in Fig. 6.

Where $I_c = G_1 V_c$ and $V_c = (\omega_d - \omega) G_{CS}$, the overall closed-loop function of the inner-loop controller is then obtained from Fig. 6 as:

$$\omega_p = \frac{G_{CS} K_C G_1 G_2}{1 + G_{CS} K_C G_1 G_2}\omega_d - \frac{G_2}{1 + G_{CS} K_C G_1 G_2} T_{DB} - \frac{G_2}{1 + G_{CS} K_C G_1 G_2} D_P (P_a - P_b) \tag{5}$$

Note that increasing G_{CS} reduces the effect of the dead-band caused by T_{DB}.

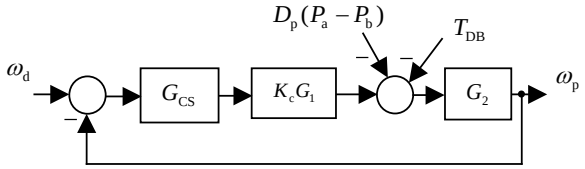

Fig. 6: *Inner-loop controller block diagram*

5.3 Flow and Pressure Characteristics

A bi-directional gear pump is used in the EHA design. During normal operation, the case drain flow will have negligible effect on the dynamic performance of EHA and the pump model may be simplified to the following, Watton (1989):

$$Q_a = D_p \omega_p - \xi(P_a - P_b) - \frac{V_a}{\beta_e}\frac{dP_a}{dt} \tag{6}$$

$$Q_b = D_p \omega_p - \xi(P_a - P_b) + \frac{V_b}{\beta_e}\frac{dP_b}{dt} \tag{7}$$

Where, pipe elasticity is included in the effective bulk modulus β_e.

EHA requires a symmetrical actuator in order to ensure flow balance between the actuator and the pump. As discussed in the previous section, a symmetrical linear actuator is specifically designed for EHA. Referring to Fig. 4, the mathematical model of this actuator is described by the following flow equations, Merrit (1967):

$$Q_1 = A\dot{x} + \frac{(V_{o_{ac}} + Ax)}{\beta_e}\frac{dP_1}{dt} + LP_1 \tag{8}$$

$$Q_2 = A\dot{x} - \frac{(V_{o_{ac}} - Ax)}{\beta_e}\frac{dP_2}{dt} - LP_2 \tag{9}$$

A small bladder-type accumulator is used to prevent:

- cavitation, and
- excessive pressure build up in the pump.

The model used for this sub-circuit is reported in Habibi and Goldenberg (1999a). During normal operation, the dynamic significance of the accumulator flow and any external leakage at the pump ports can be assumed negligible, resulting to a simplification of the model using $Q_a = Q_1$ and $Q_b = Q_2$. Given that the in/out flow from the pump is equal to the out/in flow of the actuator due to the symmetry of EHA, the load flow, Q_L, is obtained as:

$$Q_L = \frac{Q_1 + Q_2}{2} = \frac{Q_a + Q_b}{2} \tag{10}$$

In the prototype, the filtering sub-circuit is not implemented. Due to the symmetry of EHA, the pump/actuator pipe connection is modeled as a pressure drop P_{pipe}, which is a function of flow. In the prototype of EHA, P_{pipe} is approximately modeled by using Darcy's pipe flow equation as:

$$P_{pipe} \approx K_{pipe} Q_L^2 \approx K_{pipe} D_p^2 \omega_p^2 \tag{11}$$

In a linearized form:

$$\Delta P_{pipe} \approx 2K_{pipe} D_p^2 \, \Delta\omega_p \tag{12}$$

The relationship between the pump port pressures and actuator chamber pressures can be approximated to: $P_a = P_1 + P_{pipe}$, $P_b = P_2 - P_{pipe}$.

5.4 Overall Linearized Model

Substituting from the pump and actuator flow Eq. (6) to (10), neglecting the leakage flow through the case drain during normal operation and assuming that due to the symmetry of EHA $V_a \approx V_b$, the following is obtained:

$$A\ \dot{x} + \frac{V_{o_{ac}}}{2\beta_e}\left(\frac{dP_1}{dt} - \frac{dP_2}{dt}\right) + \frac{Ax}{2\beta_e}\left(\frac{dP_1}{dt} + \frac{dP_2}{dt}\right) + \frac{L}{2}(P_1 - P_2) = D_p\omega_p - \frac{V_a}{2\beta_e}\left(\frac{dP_a}{dt} - \frac{dP_b}{dt}\right) - \xi(P_a - P_b) \tag{13}$$

Since $\frac{dP_a}{dt} \approx \frac{dP_1}{dt}$ and $\frac{dP_b}{dt} \approx \frac{dP_2}{dt}$, and due to the symmetry of the actuator $\frac{dP_1}{dt} \approx -\frac{dP_2}{dt}$, for $V_o = V_{o_{ac}} + V_a$, a simplified pump/actuator model is obtained as:

$$D_p\,\omega_p = A\ \dot{x} + \frac{V_o}{\beta_e}\left(\frac{dP_1}{dt} - \frac{dP_2}{dt}\right) + \xi(P_1 - P_2) + 2\xi\, P_{pipe} + \frac{L}{2}(P_1 - P_2) \tag{14}$$

The prototype of EHA is connected to a horizontal sliding mass *M* with damping of *B*. The displacement of the mass can be related to the output force by $F = (P_1 - P_2)A = M\,\ddot{x} + B\,\dot{x}$. Substituting $(P_1 - P_2)$ by $(M\,\ddot{x} + B\,\dot{x})/A$, and rearranging, the transfer function of the hydraulic part $G_h(s)$ is obtained as:

$$G_h(s) = \frac{x(s)}{\omega_p(s)} = \frac{D_p(1 - 4K_{pipe}D_p\xi)}{E_3 + E_2 + E_1} \tag{15}$$

with

$$E_3 = s^3\left(\frac{MV_o}{\beta_e A}\right)$$

$$E_2 = s^2\left(\frac{LM/2 + \xi M + BV_o/\beta_e}{A}\right)$$

$$E_1 = s\left(\frac{A^2 + LB/2 + \xi B}{A}\right)$$

This transfer function describes the hydraulic system and can be presented in a general form as:

$$G_h = \frac{\kappa_h\,\omega_{n_h}^2}{s(s^2 + 2\zeta_h\,\omega_{n_h}\,s + \omega_{n_h}^2)} \tag{16}$$

where:

$\omega_{nh} = \sqrt{\left(\frac{A^2 + LB/2 + \xi B}{MV_o}\right)\beta_e}$ is the hydraulic undamped natural frequency,

$\zeta_h = \left(\frac{LM/2 + \xi M + BV_o/\beta_e}{2\ \omega_{n_h} M V_o}\right)\beta_e$ is the hydraulic damping ratio, and

$\kappa_h = \frac{D_p(1 - 4K_{pipe}D_p\,\xi)A}{A^2 + LB/2 + \xi B}$ is the hydraulic system gain.

The hydraulic system gain is therefore proportional to the ratio of the pump displacement over piston area. Furthermore, since in practice $4K_{pipe}\,D_p\,\xi << 1$ and $LB/2 + \zeta B << A^2$, the hydraulic system gain κ_h can be approximated to $\kappa_h = D_p/A$. This can be confirmed intuitively and indicates that a faster system response can be obtained by a higher pump displacement. Using an outer loop position controller such that input, $\omega_d = K_{pos}(x_d - x)$ and substituting:

- ω_p from Eq. (3) in (14),
- $(P_1 - P_2)$ by $(M\,\ddot{x} + B\,\dot{x})/A$, and
- rearranging, where:

$$DEN(s) = s^3\left((1 + G_{CS}K_C G_1 G_2)\frac{M\,V_o}{\beta_e A}\right) + s^2\left((1 + G_{CS}\,K_C\,G_1 G_2)\left(\frac{LM/2 + \zeta M + BV_o/\beta_e}{A}\right) + M\,G_2 D_p^2/A\right) + s\left((1 + G_{CS}K_C G_1 G_2)\left(\frac{A^2 + LB/2 + \zeta B}{A}\right) + G_2 B D_p^2/A\right) + D_p\,G_{CS}\,K_C\,G_1 G_2\,K_{pos} \tag{17}$$

the following model is obtained :

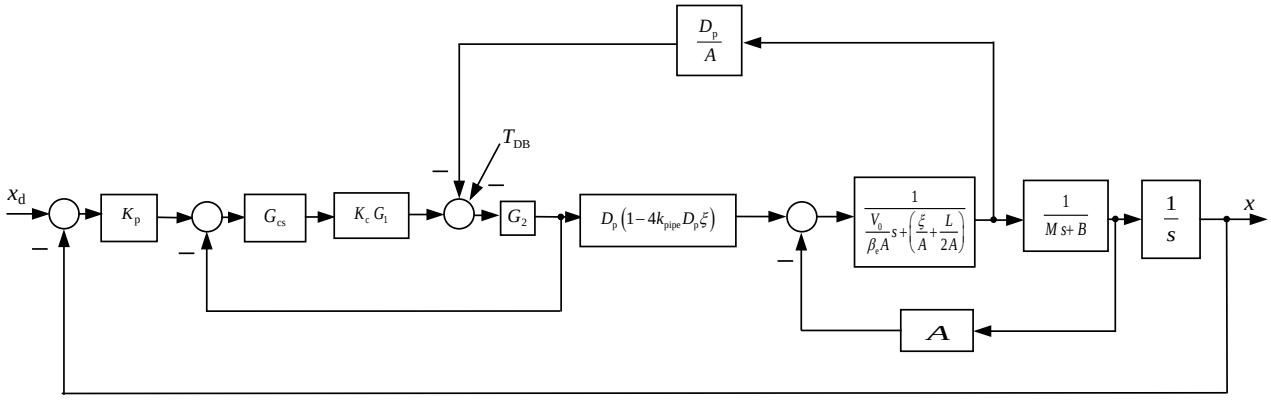

Fig. 7: *Linearized EHA model block diagram*

$$x = \frac{D_p G_{CS} K_C G_1 G_2 K_{pos} x_d}{DEN(s)} - \frac{G_2 D_p T_{DB} + (1 + G_{CS} K_C G_1 G_2) 2\xi P_{pipe} + 2P_{pipe} G_2 D_p^2}{DEN(s)} \quad (18)$$

Substituting P_{pipe} by its linearized form, a linearized mathematical model of EHA may be summarized by the block diagram in Fig. 7.

6 Design Parameters and their Link to Performance

EHA can be of value in a number of industrial sectors. Its use in Aerospace Flight Surface Actuation is consistent with the thrust of the aerospace industry towards more electric airplanes that do not use centralized hydraulic systems. This actuation system could be used to replace conventional hydraulic systems in aircraft actuation and electric actuation in missile systems. As weight distribution is a major consideration in aerospace systems, EHA can have a substantial impact on this industry. Another important application of EHA is in the robotics industry that increasingly requires modularity, high force/mass ratio, and high precision. In the context of robotics, modularity implies producing actuation systems that are both mechanically and functionally self-contained and can be assembled in various configurations to build mechanisms such as robots. Typically, a module would consist of an electronic controller, an actuator, software, sensors, and mechanical linkage. Design modularity is now confined to small, low payload manipulators that use electrical actuation. The force to mass ratio of electrical motors is poor and approximately 10 to 30 times less than hydraulic actuators at the actuation point, Hunter (1985). Heavy-duty manipulators therefore use hydraulic actuation that reduces their overall size and weight. Hydraulic systems are centralized and cannot be modularized due to their requirement of having a large oil reservoir. Therefore, there are virtually no modular heavy-duty manipulators due to the lack of an actuation system that combines modularity with provision of a high force to mass ratio. A detached configuration of EHA provides that option.

In this paper, the design parameters that impact EHA's performance are considered and quantified. These may be summarized as follows:

- maximum output force,
- maximum speed,
- configuration,
- stroke,
- motor electric time constant,
- inner-loop control gain,
- accuracy,
- hydrostatic circuit time constant, and
- outer-loop controller gain and performance.

The impact of the above design considerations on EHA's dynamic characteristics can be analyzed by using the linearized mathematical function of Eq. (18). The design parameters of the transfer function in Eq. (18) may be divided into two categories according to the following:

- **Direct:** parameters that are physically tangible and directly accessible by the designer.
- **Indirect:** parameters that are difficult to determine due to their susceptibility to environmental conditions and structural configurations.

Category 1 or direct parameters may be used for design trade-off and performance optimization. The category 2 or indirect parameters may be influenced by the designer and their effect may be analyzed by establishing upper/lower bounds for their values. In the following sections a set of mathematical functions are derived for linking performance to design parameters.

6.1 Maximum Output Force and Maximum Speed

Static characteristics of the system can determine a number of design aspects. For example, EHA may be required to move a nominal mass M at a maximum speed v_{max} subject to disturbances that would require a maximum output force of F_{max}. Where P_{max} is the maximum system pressure, the derived design parameters are:

$$A \geq F_{max} / P_{max} \quad (19)$$

$$D_p \geq v_{max} A / \omega_{max} \quad (20)$$

Note that A and D_p are oversized in Eq. (19) and (20) in order to compensate for uncertainties in friction and leakage effects within the system.

6.2 Configuration and Stroke

The stroke length x_{max} and the separation of the supply unit from the actuator, d_{sep}, are determined by the application and the physical constraints on the actuation system. These in turn determine the mean volume such that:

$$V_o = V_{o_{ac}} + V_a \tag{21}$$

where $V_{o_{ac}} = \frac{Ax_{max}}{2} + d_{sep}A_{tube} + V_{residual}$.

6.3 Electrical Time Constant of the Motor

To obtain the dominant dynamic characteristics of EHA, a review of its mathematical model would reveal possible reductions in the order of this model. The electrical and the mechanical time constants of the motor are likely to be significantly faster than the remaining time constants of the system which are in this case dominated by the hydrostatic circuit. From Eq. (16), the pertaining design requirement may be stated as:

$$100 \cdot \max(\tau_e, \tau_m) < \tag{22}$$

($\zeta_h \omega_{n_h}$ = time constant of the hydraulic circuit)

This renders the dynamics of G_1 and G_2 insignificant compared to the dynamics of the hydraulic circuit, and allows their simplification from $G_1 = \frac{K_e}{\tau_e s + 1}$ to $G_1 \approx K_e$ and, from $G_2 = \frac{K_m}{\tau_m s + 1}$ to $G_2 \approx K_m$.

6.4 Inner-Loop Speed Controller Characteristics

The gain of the inner-loop controller, its dynamic complexity and its speed of response have a large impact on the dynamic performance of EHA. The objective of the inner-loop controller is to provide accurate flow control and to ensure that the speed of response of the motor/pump subsystem remain significantly faster than that of the hydraulic circuit such that Eq. (22) is satisfied. Given the condition of Eq. (22) and the simplifications of G_1 and G_2, the transfer function relating the demanded pump speed to the actual pump speed can be obtained from Eq. (5) as:

$$G_{pm} = \frac{G_{CS}K_C G_1 G_2}{1 + G_{CS}K_C G_1 G_2} \approx \frac{G_{CS}K_C K_e K_m}{1 + G_{CS}K_C K_e K_m} \tag{23}$$

For high control gains G_{CS} such that $K_C K_e K_m G_{CS} >> 1$ Eq. (23) simplifies to the following:

$$G_{pm} = \frac{G_{CS}K_C G_1 G_2}{1 + G_{CS}K_C G_1 G_2} \approx 1 \tag{24}$$

Note that in designing G_{CS} the stability requirements of the inner-loop should also be considered.

6.5 Accuracy

The accuracy of our system is affected by the performance of the pump-speed controller at low angular velocities and its effectiveness in dealing with T_{DB}. The pump-speed control accuracy is determined by the resolution and accuracy of the speed sensor used for feedback measurement. The highest accuracy possible by the controller would be equal to the sensor accuracy denoted by $V_{sensor_{acc}}$ which is the smallest detectable and meaningful incremental change in output. The steady state error of the controller is then added to $V_{sensor_{acc}}$ to quantify the static performance of the pump speed controller. If there is no integral action in G_{CS} (i.e. the steady state error of the motor controller is not equal to zero), the steady-state error of the controller is quantified by $\left(1 - \frac{G_{CS}K_C K_e K_m}{1 + G_{CS}K_C K_e K_m}\right) V_{sensor_{acc}}$. The accuracy of the pump-speed controller at its lowest angular velocity is then given by:

$$\Omega_p = \left(1 + 1 - \frac{G_{CS}K_C K_e K_m}{1 + G_{CS}K_C K_e K_m}\right) V_{sensor_{acc}} \approx 2V_{sensor_{acc}} \tag{25}$$

If integral action is included in G_{CS} such that $G_{CS} = K_{P_{CS}} + \frac{K_{I_{CS}}}{s}$, the accuracy of the pump-speed controller becomes equal to the sensor accuracy:

$$\Omega_p = V_{sensor_{acc}} \tag{26}$$

The positional accuracy (Acc_{DB}) can be calculated for $s = j0$ from Eq. (18) as

$$Acc_{DB} = \frac{G_2 D_p T_{DB} + (1 + G_{CS}K_C G_1 G_2)2\xi P_{pipe} + 2P_{pipe}G_2 D_p^2}{D_p G_{CS}K_C G_1 G_2 K_{pos}}.$$

If integral action is added to G_{CS} such that $G_{cs} = K_{P_{CS}} + \frac{K_{I_{CS}}}{s}$ then Acc_{DB} is reduced to $Acc_{DB} = 2\xi P_{pipe} / D_p K_{pos}$. From Eq. (11), P_{pipe} can be modeled as $K_{pipe}Q_L^2 \approx K_{pipe}D_p^2\omega_p^2$ and the expected positional accuracy is obtained as:

$$Acc_{DB} = 2\xi K_{pipe} D_p \Omega_p^2 / K_{pos} \tag{27}$$

This is true provided that the theoretical effect of the dead-band and the pressure drop across components on the positional accuracy of EHA is greater than the accuracy of the position sensor $P_{sensor_{acc}}$. The outer-loop maximum position control accuracy is then stated as:

$$Acc = \max(P_{sensor_{acc}}, Acc_{DB}) \tag{28}$$

If the design requirement for accuracy is specified to be within a range Acc_{min} and Acc_{max}, then the equation linking design parameter to performance pertaining to accuracy can be stated as:

$$Acc_{min} \le \min(P_{sensor_{acc}}, Acc_{DB}) \le Acc_{max} \tag{29}$$

The implication of the above equation is that the

dead-band is minimized by the inner/outer loop control strategy and careful selection of components. It can be concluded from this equation that, in designing EHA, the following rules apply:

- the inner loop control strategy can alleviate the dead-band at the pump/motor interface,
- selection of the pump impacts the effect of the dead-band influenced by pressure drop of components situated between the pump and the actuator,
- the selection of the pump is made on the basis of the values of ξ and D_p, and
- the outer-loop position controller for $K_{pos} > 1$ reduces the effect of dead-band influenced by pressure drop of components situated between the pump and the actuator.

6.6 Outer-Loop Dynamic Response

There are a multitude of strategies for designing EHA. In this section, two cases are considered.

Case 1: Very large inner-loop gain

In this analysis it is assumed that the choice of the electric motor allows setting of very large inner-loop gains. If the effect of T_{DB} is assumed to be negligible due to the inner-loop control strategy, the block diagram of Fig. 7 can be expressed in terms of the electric motor and hydraulic transfer functions as shown in Fig. 8. The electric motor transfer function is obtained from Eq. (23) and the hydraulic transfer function is defined by Eq. (15).

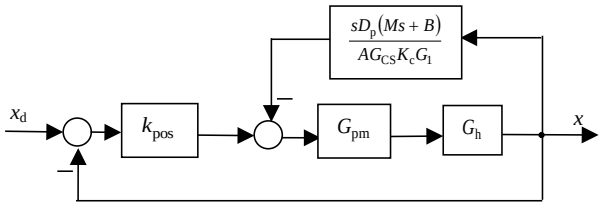

Fig. 8: *Linearized EHA model block diagram*

Many factors affect the dynamic performance of EHA. The most suitable design strategy is to use a high gain inner-loop controller and a motor that is fast enough to allow the approximation of G_{pm} to $G_{pm} \approx 1$ as discussed in section 6.4. Furthermore, for large inner-loop gains, the dynamic significance of the term $\frac{s\,D_p\,(Ms+B)}{AG_{CS}\,K_c\,G_1}$ can become negligible and, a simplified transfer function for our system can then be expressed as:

$$T(s)=\frac{x(s)}{x_d(s)}=\frac{\kappa_h\omega_{n_h}^2 K_{pos}}{s^3+2\zeta_h\omega_{n_h}s^2+\omega_{n_h}^2 s+\kappa_h\omega_{n_h}^2 K_{pos}}$$

$$=\frac{D_p(1-4K_{pipe}D_p\xi)K_{pos}}{DEN_T(s)}$$

where

$$DEN_T(s)=s^3\left(\frac{MV_o}{\beta_e A}\right)+s^2\left(\frac{LM/2+\zeta M+BV_o/\beta_e}{A}\right)$$

$$+s\left(\frac{A^2+LB/2+\zeta B}{A}\right)+D_p(1-2K_{pipe}D_p)K_{pos} \qquad (30)$$

The hydraulic model G_h considers the slippage of the pump and the leakage from the actuator. These effects affect the accuracy of the system as shown by Eq. (18) and (27). Their impact on the dynamic performance of the system in terms of gain and natural frequency is however negligible as $\xi << A$ and $L << A$. Furthermore, since $4K_{pipe}\,D_p\,\xi << 1$, the term $(1 - 4\,K_{pipe}\,D_p\,\xi)$ can be approximated to 1. Referring to Eq. (30), the expressions for hydraulic gain and natural frequency may be simplified to the following:

$$\omega_{n_h}=\sqrt{\left(\frac{A^2+LB/2+\zeta B}{MV_o}\right)\beta_e}\approx\sqrt{\left(\frac{A^2\beta_e}{MV_o}\right)} \qquad (31)$$

$$\kappa_h=\frac{D_p\left(1-2K_{pipe}D_p\right)A}{A^2+LB/2+\xi B}\approx\frac{D_p}{A} \qquad (32)$$

For $\beta_e >> 1$, the hydraulic damping factor may be simplified to:

$$\zeta_h=\left(\frac{LM/2+\xi M+BV_o/\beta_e}{2\omega_{n_h}MV_o}\right)\beta_e\approx\left(\frac{LM/2+M\xi}{2\omega_{n_h}MV_o}\right)\beta_e \qquad (33)$$

The overall closed loop transfer function of equation (30) may then be simplified to the following:

$$T(s)=\frac{x(s)}{x_d(s)}\approx\frac{\frac{D_pA}{V_oM}K_{pos}}{\frac{1}{\beta_e}s^3+\frac{L/2+\xi}{V_o}s^2+\frac{A^2}{V_oD_pM}s+\frac{D_pA}{V_oM}K_{pos}} \qquad (34)$$

The philosophy of system design is to establish a simple correlation between the system parameters and the characteristic roots of transfer function $T(s)$ so that the roots may be set at desired locations by adjusting the system parameters and controller gains. The parameter plane analysis can be used for analyzing Eq. (34) and for selection of components for EHA. The objective here is to determine, whether the chosen components can provide the desired dynamic response. For design trade off, the characteristic polynomial of $T(s)$, referred to as $DEN_T(s)$ may be determined in terms of variables $\alpha=\frac{D_p\,A}{V_o\,M}K_{pos}$ and $\chi=\frac{A^2}{M}$ made up of category 1 parameters such that from Eq. (34):

$$DEN_T(s)=\frac{1}{\beta_e}s^3+\frac{(L/2+\xi)}{V_o}s^2+\frac{1}{V_o}\chi\quad s+\alpha \qquad (35)$$

Note that the variable α is a function of the outer-loop gain K_{pos}, which can be adjusted to compensate for changes in D_p, V_0 or M. Parameter mapping enables us to link α and χ to the desired dynamic performance of our system. The mapping is used to transform points from the complex s-plane onto the parameter $\alpha\,\chi$ plane, Siljak (1969). In our case, the function is third order such that:

$$DEN_T(s)=\sum_{i=0}^{3}a_i\,s^i=0 \qquad (36)$$

where s is the complex variable $s = \alpha\sigma + j\omega$ and the coefficients a_i are functions of α and χ. Substituting the complex variable s in our characteristic equation, then Eq. (36) can be rewritten as a system of two simultaneous equations:

$$R \equiv \sum_{i=0}^{3} a_i X_i = 0 \tag{37}$$

$$I \equiv \sum_{i=0}^{3} a_i Y_i = 0 \tag{38}$$

Where, substituting for s:

$$\bar{X} = \{X_0, X_1, X_2, X_3\} = \{\ 1,\ \sigma,\ \sigma^2 - \omega^2,\ \sigma^3 - 3\omega^2\sigma\} \tag{39}$$

$$\bar{Y} = \{Y_0, Y_1, Y_2, Y_3\} = \{\ 0,\ \omega,\ 2\sigma\omega,\ 3\omega\sigma^2 - \omega^3\} \tag{40}$$

Referring to Eq. (35), the coefficients a_i are functions of α and χ, and can be expressed in the form:

$$a_i = b_i\,\alpha + c_i\,\chi + d_i \ \text{ for } (i = 0,..,3) \tag{41}$$

The four coefficients of Eq. (36) are obtained as:

$$a_0 = b_0\,\alpha + c_0\,\chi + d_0 = \alpha$$

$$a_1 = b_1\,\alpha + c_1\,\chi + d_1 = \left(\frac{1}{V_o}\right)\chi$$

$$a_2 = b_2\,\alpha + c_2\,\chi + d_2 = \frac{(L/2+\xi)}{V_o}$$

$$a_3 = b_3\,\alpha + c_3\,\chi + d_3 = \frac{1}{\beta_e}$$

Giving:

$$\bar{b} = \{b_0,..,b_3\} = \{1,\ 0,\ 0,\ 0\} \tag{42}$$

$$\bar{c} = \{c_0,..,c_3\} = \left\{0, \left(\frac{1}{V_o}\right), 0, 0\right\} \tag{43}$$

$$\bar{d} = \{d_0,..,d_3\} = \left\{0,\ 0, \frac{(L/2+\xi)}{V_o}, \left(\frac{1}{\beta_e}\right)\right\} \tag{44}$$

Substituting from Eq. (39) to (44), Eq. (37) and (38) can be rewritten as:

$$\alpha B_1 + \chi C_1 + D_1 = 0 \tag{45}$$

$$\alpha B_2 + \chi C_2 + D_2 = 0 \tag{46}$$

Where, substituting from (39), (40), (42), (43) and (44):

$$B_1 = \sum_{i=0}^{3} b_i X_i = 1 \tag{47}$$

$$B_2 = \sum_{i=0}^{3} b_i Y_i = 0 \tag{48}$$

$$C_1 = \sum_{i=0}^{3} c_i X_i = \sigma\left(\frac{1}{V_o}\right) \tag{49}$$

$$C_2 = \sum_{i=0}^{3} c_i Y_i = \omega\left(\frac{1}{V_o}\right) \tag{50}$$

$$D_1 = \sum_{i=0}^{3} d_i X_i = \left(\frac{1}{\beta_e}\right)(\sigma^3 - 3\omega^2\sigma) + \frac{(L/2+\xi)}{V_o}(\sigma^2 - \omega^2) \tag{51}$$

$$D_2 = \sum_{i=0}^{3} d_i Y_i = \left(\frac{1}{\beta_e}\right)(3\omega\sigma^2 - \omega^3) + \frac{(L/2+\xi)}{V_o} 2\omega\sigma \tag{52}$$

Equations (45) and (46) may be solved for unknowns α and χ such that:

$$\alpha = \frac{C_1 D_2 - C_2 D_1}{B_1 C_2 - B_2 C_1} \tag{53}$$

$$\chi = \frac{B_2 D_1 - B_1 D_2}{B_1 C_2 - B_2 C_1} \tag{54}$$

for $B_1 C_2 - B_2 C_1 \neq 0$.

Our linearized third order equation can be expressed as the summation of a first and second order system by using partial fraction decomposition as follows:

$$T(s) \Rightarrow \left(\frac{\kappa_1}{s + p_1} + \frac{\kappa_2 s + \kappa_3}{s^2 + 2\zeta\omega_n s + \omega_n^2}\right) \tag{55}$$

The three poles of our transfer function are therefore $s = -\zeta\omega_n \pm j\omega_n\sqrt{1-\zeta^2}$ and $s = -p_1$. To relate α and χ to our damping coefficient and natural frequency, substitution of s by $s = -\zeta\omega_n \pm j\omega_n\sqrt{1-\zeta^2}$ is equivalent to letting $\sigma = -\omega_n\,\zeta$ and $\omega = \omega_n\sqrt{1-\zeta^2}$. Substituting σ and ω in Eq. (47) and (52), the parameters α and χ can be obtained from Eq. (53) and (54) as:

$$\alpha = \left(\frac{(L/2+\xi)}{V_o} - \frac{2\zeta\omega_n}{\beta_e}\right)\omega_n^2 \tag{56}$$

$$\chi = \frac{\left(\left(\omega_n\sqrt{1-\zeta^2}\right)^2 - 3\left(\zeta\omega_n\right)^2\right)}{\beta_e} + 2\zeta\,\omega_n\left(L/2+\xi\right) \tag{57}$$

A range of values for ζ and ω_n can now be used for specifying boundaries for design trade off in α and χ,. For example for ζ = 0.7 and $\omega_{n\,max} \geq \omega_n \geq \omega_{n\,min}$ the pertinent requirement on α and χ can be stated as follows.

$$\chi_{min} \leq \chi \leq \chi_{max} \tag{58}$$

$$\alpha_{min} \leq \alpha \leq \alpha_{max} \tag{59}$$

Where χ_{min} , χ_{max} , α_{min} and α_{max} are the minimum and maximum values of α and χ corresponding to

ω_{nmin} and ω_{nmax}. Note that $\alpha = \frac{D_p A}{V_o M} K_{pos}$ and that the value of α is adjusted in response to χ by changing the outer-loop position gain K_{pos}. For a chosen value of χ, the derived requirement (59) may now be revised in terms of K_{pos} as follows:

$$\frac{V_o M \alpha_{min}}{D_p A} \le K_{pos} \le \frac{V_o M \alpha_{max}}{D_p A} \quad (60)$$

Case 2: Design trade off between inner-loop and outer-loop gains

In the case where the assumptions of case 1 are not valid, i.e. for example $\frac{s D_p (M s + B)}{A G_{CS} K_c G_1}$ is dynamically significant, then the more complete model of EHA needs to be considered. Referring to Fig. 7, since $\xi << A$ and $L << A$, the transfer function $\frac{1}{\frac{V_o}{\beta_e A} s + \left(\frac{\xi}{A} + \frac{L}{2A}\right)}$ can be simplified to $\frac{\beta_e A / V_o}{s}$.

The overall simplified input/output transfer function, given the outer-loop position controller can be obtained as:

$$T(s) = \frac{K_{pos} G_{CS} K_c K_m K_e (D_p - 4 K_{pipe} \xi D_p^2) \beta_e A}{DEN_T(s)} \quad (61)$$

where,

$$\begin{aligned} DEN_T(s) = & \left(M(1 + G_{CS} K_c K_m K_e)/V_o\right) \; s^3 \\ & + ((M K_m (D_p - 4 K_{pipe} \xi D_p^2) \beta_e D_p \\ & + B(1 + G_{CS} K_c K_m K_e)/V_o) \beta_e D_p) s^2 \\ & + ((G_{CS} K_c K_m K_e \beta_e A^2) + (\beta_e A^2) \\ & + B K_m (D_p - 4 K_{pipe} D_p^2 \xi) \beta_e D_p) s \\ & + K_{pos} G_{CS} K_c K_m K_e (D_p - 4 K_{pipe} \xi D_p^2) \beta_e A \end{aligned} \quad (62)$$

If our motor control strategy uses proportional gain only, i.e. $G_{CS} = K_{PCS}$, and for $\beta_e >> 1$, Eq. (61) reduces to a second order form as follows:

$$T(s) = \frac{K_{pos} G_{CS} K_c A/(M D_p)}{DEN_T(s)} \quad (63)$$

where

$$DEN_T(s) = s^2 + \frac{G_{CS} K_c K_e - 1/K_m) A^2 + B(D_p^2 - 4 K_{pipe} \xi D_p^3}{M (D_p - 4 K_{pipe} \xi D_p^2) D_p} s + K_{pos} G_{CS} K_c A/(M D_p)$$

Equation (63) can be readily used for obtaining the desired dynamic response and, its natural frequency and damping ratio may be obtained as:

$$\omega_n = \sqrt{\frac{K_{pos} G_{CS} K_c A}{M D_p}} \quad (64)$$

and

$$\zeta = \left(\frac{(G_{CS} K_c K_e - 1/K_m) A^2 + B(D_p^2 - 4 K_{pipe} \xi D_p^3)}{2 \omega_n M (D_p - 4 K_{pipe} \xi D_p^2) D_p} \right) \quad (65)$$

The associated rise time, and settling time can be obtained as:

$$t_{rise} = \frac{1}{\omega_n \sqrt{1 - \zeta^2}} \tan^{-1} \left(- \frac{\sqrt{1 - \zeta^2}}{\zeta} \right) \quad (66)$$

$$t_{settling} = \frac{4}{\omega_n \sqrt{1 - \zeta^2}} \quad (67)$$

Equations (64) to (67) can be used for the analysis and selection of parts for EHA. The positional accuracy of the system may be improved considerably by adding integral action to the inner-loop control strategy such that $G_{CS} = K_{PCS} + K_{ICS}/s$. Substituting G_{CS} in Eq. (63) results in the following third order transfer function:

$$T(s) = \frac{(K_{P_{CS}} s + K_{I_{CS}}) K_{pos} K_c A/(D_p R_c)}{DEN_T(s)} \quad (68)$$

where,

$$\begin{aligned} DEN_T(s) = & M s^3 + \left(A^2 \frac{1 + K_c K_{P_{CS}} G_2 / R_c}{D_p (D_p - 4 K_{pipe} \xi D_p^2) G_2} + B \right) s^2 \\ & + \left(K_{pos} K_{P_{CS}} K_c A/(R_c D_p) + \frac{K_{I_{CS}} K_c A^2}{D_p (D_p - 4 K_{pipe} \xi D_p^2) R_c} \right) s \\ & + K_{pos} K_{I_{CS}} K_c A/(D_p R_c) \end{aligned}$$

Equation (63) can be used for provisional selection of components for EHA. The effect of adding integral action to the inner loop controller may be examined by using Eq. (68) and the parameter plane analysis as demonstrated for Case 1, Siljak (1969). The objective here is to determine whether the chosen components can provide the desired dynamic response. The inner-loop gains K_{PCS} and K_{ICS} are related such that $K_{PCS}/K_{ICS} = \gamma$ in accordance with the stability and performance requirements of the inner-loop control strategy, this results in K_{PCS} being defined and linked to γ and K_{ICS}. The control gains that would then be required to be determined and could be traded off are: K_{ICS} and K_{pos}. The characteristic polynomial of $T(s)$ may be determined in terms of variables $\alpha = K_{pos} K_{ICS}$ and $\chi = K_{ICS}$ such that:

$$\begin{aligned} DEN_T(s) = & M s^3 + \left(A^2 \frac{1 + K_c G_2 \gamma \chi / R_c}{D_p (D_p - 4 K_{pipe} \xi D_p^2) G_2} + B \right) s^2 \\ & + \left(\alpha \gamma K_c A/(D_p R_c) + \frac{\chi K_c A^2}{D_p (D_p - 4 K_{pipe} \xi D_p^2) R_c} \right) s \\ & + \alpha K_c A/(D_p R_c) \end{aligned} \quad (69)$$

Note that variable α is again a function of the outer-loop gain K_{pos} which can be adjusted to compensate changes K_{ICS}. As in case 1, the parameters α and χ can be obtained as:

$$\alpha = \frac{R_c D_p \omega_n^2}{AK_c} \times$$
$$\left(\frac{K_c B + K_c M \omega_n (\zeta^3 - 2\zeta)}{K_c - G_2 \omega_n (2G_2 \zeta K_c \gamma - 2\zeta R_c + \omega_n R_c \gamma + G_2 \omega_n K_c \gamma^2)} \right.$$
$$\left. + \frac{MG_2 \omega_n^2 (R_c + G_2 K_c \gamma)(1 + \zeta^2 - 2\zeta^4)}{K_c - G_2 \omega_n (2G_2 \zeta K_c \gamma - 2\zeta R_c + \omega_n R_c \gamma + G_2 \omega_n K_c \gamma^2)} \right) \quad (70)$$

$$\chi = \omega_n R_c (D_p^2 - 4K_{pipe} \xi D_p^3) \times$$
$$\left(\frac{2B\zeta - \omega_n \gamma B + \omega_n^2 \gamma M (2\zeta - \zeta^3) - 3\omega_n M \zeta^2 + \omega_n M)}{A^2 (K_c - G_2 \omega_n ((2\zeta + \omega_n \gamma) G_2 K_c \gamma - 2\zeta R_c + \omega_n R_c \gamma)} \right) \quad (71)$$

A range of values for ζ and ω_n can now be used for specifying boundaries for design trade off in α and χ such that:

$$\chi_{min} \le \chi \le \chi_{max} \quad (72)$$

$$\alpha_{min} \le \alpha \le \alpha_{max} \quad (73)$$

Where χ_{min} , χ_{max} , α_{min} and α_{max} are the minimum and maximum values of α and χ corresponding to ω_{nmin} and ω_{nmax} .

Since $\alpha \equiv K_{pos} K_{ICS}$ and the value of α is adjusted in response to χ by changing the outer-loop position gain K_{pos}, for a chosen value of $\chi \equiv K_{ICS}$, the derived requirement for K_{pos} may now be stated from Eq. (73) as:

$$\frac{\alpha_{min}}{K_{I_{cs}}} \le K_{pos} \le \frac{\alpha_{max}}{K_{I_{cs}}} \quad (74)$$

The dynamic characteristics of EHA are now linked to design parameters through a set of equations that can now be used for analysis and design optimization. The choice of case strategy depends on the application and availability of off-the-shelf components.

7 Analysis of EHA Prototype

A prototype has been produced as shown in Fig. 9. The category 1 (measured) and 2 (estimated) parameters of this prototype are listed in Tables 1 and 2 respectively. In this section, the performance of the prototype is analyzed using equations previously derived in this paper. Given the experimental nature of the prototype, the following parameters were set at the inception of design:

- maximum working pressure, P_{max} to 20700 kPa (3000 psi),
- maximum stroke of 12 cm, and
- large output force capability in excess of 10500 N.

In the following sections, the mathematical relationships derived in section 6 are applied to the EHA prototype.

7.1 Maximum Output Force and Maximum Speed

Static characteristics of the system are determined using Eq. (19) to (20). For P_{max} set to 20700 kPa, F_{max} is chosen as 10.5 kN, giving:

$$A = F_{max} / P_{max} = 5.05 \cdot 10^{-4} \text{ m} \quad (75)$$

A small commercial gear pump is used with ω_{max} = 419 rad/s resulting in a maximum saturation load velocity of:

$$v_{max} = \omega_{max} D_p / A = 0.47 \quad \text{m/s} \quad (76)$$

Fig. 9: *EHA prototype*

Table 1: Category 1 direct parameters of the prototype

Symbol	Definitions	Values
A	Pressure area in symmetrical actuators	$5.05\cdot10^{-4}$ m^2
D_{p}	Pump volumetric displacement	$5{,}73\cdot10^{-7}$ m^3/rad
J_{pm}	Motor/pump inertia	$1.6\cdot10^{-3}$ kgm^2
K_{a_1}	Conversion factor linking maximum actuator displacement to maximum motor speed	6980 rad/s/m
K_{a_2}	Conversion factor linking input to the motor to motor speed	41.87 rad/s/V
K_{c}	Motor gain	1 Nm/A
$K_{\mathrm{I_{CS}}}$	Integral gain	$2.4\cdot K_{a_2}$
$K_{\mathrm{p_{CS}}}$	Proportional gain	$1.2\cdot K_{a_2}$
K_{pos}	Outer-loop proportional gain	$1\cdot K_{a_1}$
L_{c}	Motor line to line inductance	0.004 H
M	Load mass	20 kg
$P_{\max}$	Maximum pressure in the system	20700 kPa
$P_{sensor_{acc}}$	Accuracy of position sensor	10^{-6} m
R_{c}	Motor line to line resistance	$0.5\,\Omega$
V_0	Total mean volume	$6.1\cdot10^{-5}$ m^3
$V_{sensor_{acc}}$	Accuracy of motor velocity sensor	1 rad/s
$x_{\max}$	Maximum stroke length	12 cm
τ_{e}	Time constant of the motor's electrical circuit	0.008 s
τ_{m}	Time constant of the motor's mechanical part	0.0016 s

Table 2: Estimated category 2 indirect parameters of the prototype

Symbol	Definitions	Value
B	Coefficient of friction at the load	0.5 N/m/s
$K_{p_{visc}}$	Coefficient due to viscous	$2.2\cdot10^{-3}$ Nm/rad/s
K_{pipe}	Pipe coefficient relating pressure drop to flow	$2.5\cdot10^{12}$ Pa/m^6/s^2
L	Leakage coefficient	$2.6\cdot10^{-11}$ m^3/s/Nm^{-2}
T_{DB}	Nonlinear friction (including static and coulomb) at the pump motor interface	2 Nm (Peak value)
β_{e}	Effective bulk modulus of hydraulic oil	$1.2\cdot10^{8}$ Pa
ξ	Pump cross-port leakage coefficient	$1.5\cdot10^{-11}$ m^3/s/Nm^{-2}

7.2 Configuration and Stroke

The stroke length $x_{\max}$ is set at 12 cm with the actuator placed near the pump with resulting $V_0 = 6.1\cdot10^{-5}$ m^3.

7.3 Hydraulic Transfer Function

The transfer function of the hydraulic part is specified by Eq. (15) and, for the EHA prototype is obtained as:

$$G_{\mathrm{h}}(s) = \frac{x(s)}{\omega_{\mathrm{p}}(s)}$$

$$= \frac{\kappa_{\mathrm{h}}\omega_{\mathrm{n_h}}^2}{s(s^2 + 2\zeta_{\mathrm{h}}\omega_{\mathrm{n_h}}s + \omega_{\mathrm{n_h}}^2)} \approx \frac{28}{s(s^2 + 54.5s + 24794)} \qquad (77)$$

The corresponding natural frequency, damping ratio and gain are: $\omega_{\mathrm{n\ h}} = 157$ rad/s, $\zeta_{\mathrm{h}} = 0.18$ and $\kappa_{\mathrm{h}} = 1.13\cdot10^{-3}$ m/rad/s.

7.4 Inner-Loop Speed Controller Characteristics

A high gain inner-loop controller

$$G_{\mathrm{CS}} = K_{\mathrm{P_{CS}}} + \frac{K_{\mathrm{I_{CS}}}}{s} = 50 + \frac{100}{s}$$

that includes the amplifier conversion factor $K_{\mathrm{a2}} = 21$ rad/s/V, is used for regulating the motor speed. G_{pm} is obtained as:

$$G_{\mathrm{pm}} = \frac{G_{\mathrm{CS}}\,K_{\mathrm{C}}\,G_1\,G_2}{1 + G_{\mathrm{CS}}\,K_{\mathrm{C}}\,G_1\,G_2} \approx \frac{(\gamma s + 1)}{(1/K_{\mathrm{C}}K_{\mathrm{e}}K_{\mathrm{m}}K_{\mathrm{I_{CS}}}) + \gamma)s + 1} \qquad (78)$$

where $\gamma = \dfrac{K_{\mathrm{P_{CS}}}}{K_{\mathrm{I_{CS}}}}$. The use of high inner loop gains such that $\dfrac{1}{K_{\mathrm{C}}K_{\mathrm{e}}K_{\mathrm{m}}K_{\mathrm{I_{CS}}}} << \gamma$ results in the following simplification:

$$G_{\text{pm}} = \frac{(\gamma s+1)}{((1/K_{\text{C}}K_{\text{e}}K_{\text{m}}K_{\text{I}_{\text{CS}}})+\gamma)s+1)} \approx \frac{(\gamma s+1)}{(\gamma s+1)} = 1 \quad (79)$$

In this case where $\gamma = \frac{K_{\text{P}_{\text{CS}}}}{K_{\text{I}_{\text{CS}}}} = 0.5$, the transfer function relating the demanded pump speed to the actual pump speed for the prototype can be accordingly simplified to:

$$G_{\text{pm}} = \left(\frac{(\gamma s+1)}{((1/K_{\text{C}}K_{\text{e}}K_{\text{m}}K_{\text{I}_{\text{CS}}})+\gamma)s+1)} = \frac{(0.5s+1)}{(0.52s+1)} \right) \quad (80)$$

7.5 Accuracy

From Eq. (26) and due to integral action in G_{CS}, the pump-speed control accuracy is determined by the resolution and accuracy of the speed sensor used for feedback measurement which is: $\Omega_{\text{p}} = V_{sensor_{acc}} = 1$ rad/s.

An optical encoder with an accuracy of $P_{sensor_{acc}} = 10^{-5}$ is used for position measurement. The positional accuracy of EHA estimated from linear analysis is obtained from Eq. (28) as:

$$\begin{aligned} Acc &= \max(P_{\text{sensor}_{\text{acc}}}, Acc_{\text{DB}}) \\ &= \max(P_{\text{sensor}_{\text{acc}}}, 2\xi K_{\text{pipe}} D_{\text{p}} \Omega_{\text{p}} / K_{\text{pos}}) \\ &= \max(10^{-5}, 6\cdot 10^{-11}) = 10^{-5}\,\text{m} \end{aligned} \quad (81)$$

7.6 Outer-Loop Dynamic Response

The hydraulic and electric motor transfer functions of Eq. (77) and (80) in conjunction with the parameters of Tables 1 and 2, are used for simulating the model of Fig. 8. The simulated response of the system is given in Fig. 10 and closely matches the actual response of Fig. 11. Note that the model is only required to predict the significant dynamics of the system at the design stage. The full mathematical model may be then used for detailed analysis if required.

The overall transfer function of EHA can be approximated to Eq. (34). Substituting values from Tables 1 and 2:

$$\begin{aligned} T(s) &= \frac{x(s)}{x_{\text{d}}(s)} = \frac{\kappa_{\text{h}}\omega_{\text{n}_{\text{h}}}^2 K_{\text{pos}}}{s^3 + 2\zeta_{\text{h}}\omega_{\text{n}_{\text{h}}}s^2 + \omega_{\text{n}_{\text{h}}}^2 s + \kappa_{\text{h}}\omega_{\text{n}_{\text{h}}}^2 K_{\text{pos}}} \\ &\approx \frac{1.96\times 10^5}{(s+8)(s^2+46.48s+2442)} \end{aligned} \quad (82)$$

Note that the dominant characteristic in this case is the real root at s = -8. The simulated response of this system (Fig. 10) demonstrates a 0 to 90 % rise time of 0.3 seconds and a settling time of 0.5 seconds, which is the same as the prototype. The actual performance of the prototype closely matches its expected performance as compared in Table 3.

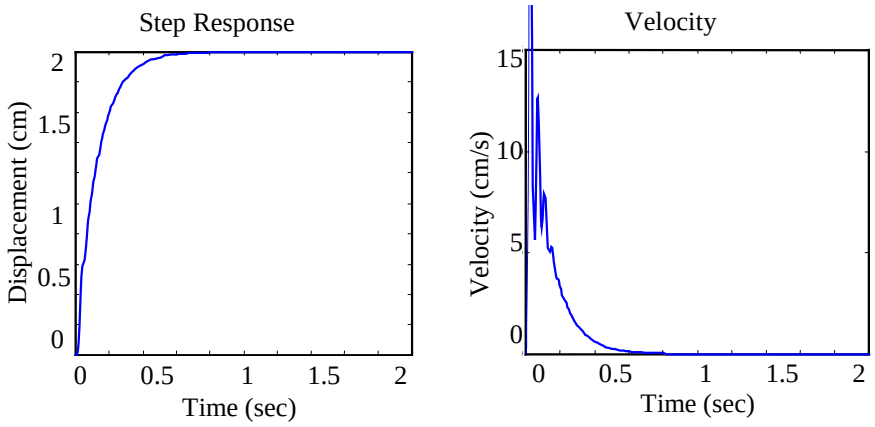

Fig. 10: *Simulated response of the EHA prototype*

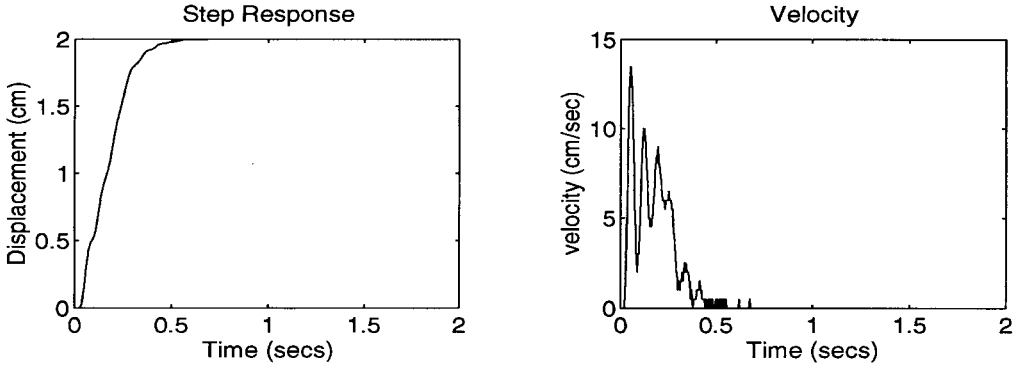

Fig. 11: *Measured step response of the EHA prototype*

Table 3: Comparison of simulated versus actual performance of the EHA prototype

Symbol	Definitions	Simulated value	Actual value
Acc	Positional accuracy (load of 20 kg)	10 Micron	10 Micron
$F_{\max}$	Maximum output force	10.5 kN	10.5 kN
t_{rise}	Rise time (load of 20 kg)	0.3 s	0.3 s
t_{settling}	Settling time (load of 20 kg)	0.5 s	0.5 s
$X_{\max}$	Maximum stroke	0.12 m	0.12 m

Table 4: Performance indicators

Performance indicator	Prototype	Constraints (range)	Demanded or target value	Optimized value
Accuracy (m)	0.00001	$0 \rightarrow 0.0001$	Less than 0.00001	0.00001
Maximum Output Force (N)	10500	$3000 \rightarrow 11550$	10500	9680
Maximum Speed (m/s)	0.47	$0.15 \rightarrow 1.0$	0.47	0.47
M (kg)	20	$10 \rightarrow 100$	20	15.8
$p_1(s)$	8	$8 \rightarrow 170$	20	20
α	$2.9 \cdot 10^{-4}$	$-0.1039 \rightarrow 0.016$	-0.0122	$4 \cdot 10^{-4}$
χ	$4 \cdot 10^{-6}$	$-0.001 \rightarrow 3.4 \cdot 10^{-4}$	$8.54 \cdot 10^{-9}$	$3.4 \cdot 10^{-6}$

Table 5: Direct or category 1 parameter used in design trade-off

Design parameters used in optimization	Prototype	Range	Optimized value
$D_p(\text{m}^3/\text{rad})$	$5.73 \cdot 10^{-7}$	$1.15 \cdot 10^{-7} \rightarrow 57.3 \cdot 10^{-7}$	$14.09 \cdot 10^{-7}$
$A(\text{m}^2)$	$5.05 \cdot 10^{-4}$	$0.1 \cdot 10^{-4} \rightarrow 10 \cdot 10^{-4}$	$4.66 \cdot 10^{-4}$
K_{pos} (rad/s/m)	$1 \cdot K_{a_1}$	$0.11 \cdot K_{a_1} \rightarrow 2.1 \cdot K_{a_1}$ $1 \cdot K_{a_1}$	$0.92 \cdot K_{a_1}$
ω_n (rad/s)	49.42	$20 \rightarrow 170$	49.17
ζ	0.47	$0.4 \rightarrow 0.9$	0.474
M (kg)	20	$10 \rightarrow 100$	15.8
$P_{\max}$ (kPa)	20700	$7000 \rightarrow 30000$	20750

8 Design Improvement

The performance of the prototype may be quantified by a set of indicators as derived in section 6 and as listed in Table 4. The prototype is not optimal with respect to these performance indicators. In any design, the performance requirements are specified to within a range. Given this range, numerical optimization could be used to improve performance. An illustrative example is provided in this section.

The EHA prototype satisfies the condition of Eq. (80) and, its dominant dynamic characteristics are captured by the transfer function of Eq. (82). Note that the dominant characteristic in this case is the real root at $s = -p_1 = -8$ and, the speed of response can be improved by moving this pole further into the left half plane. If a range is set for the performance indicators of the prototype as given in Table 4, the design may be optimized for this range by using numerical optimization. The parameters in Table 5 are used for design trade off according to the mathematical functions that link performance and design parameters. Here, case 1 condition is assumed as detailed in section 6.6.

The following cost function C and the constraints of Table 4 are used for increasing the response time of the system through numerical optimization:

$$C = \left(\frac{\alpha_{\text{dem}} - \alpha}{\alpha_{\max} - \alpha_{\min}}\right)^2 w_1 + \left(\frac{\chi_{\text{dem}} - \chi}{\chi_{\max} - \chi_{\min}}\right)^2 w_2 + \left(\frac{P_{1_{\text{dem}}} - P_1}{P_{1\max} - P_{1\min}}\right)^2 w_3 + \left(\frac{Acc_{\text{dem}} - Acc}{Acc_{\max} - Acc_{\min}}\right)^2 w_4 + \left(\frac{F_{\max_{\text{dem}}} - F_{\max}}{F_{\max_{\max}} - F_{\max_{\min}}}\right)^2 w_5 + \left(\frac{V_{\max_{\text{dem}}} - V_{\max}}{V_{\max_{\max}} - V_{\max_{\min}}}\right)^2 w_6 + \left(\frac{M_{\text{dem}} - M}{M_{\max} - M_{\min}}\right)^2 w_7 \quad (83)$$

Where the minimum, maximum and demanded (or target) values used in the calculation of the cost function are listed in Table 5. Since this is a multi-objective

optimization problem, prioritization is made through weights such that:

$w_1 = 1$, $w_2 = 1$, $w_3 = 1$, $w_5 = 1$, $w_6 = 1$, $w_7 = 1$ and $w_4 = 1$ for $Acc > 10^5$ else $w_4 = 0$. Note that given these weights, the terms of Eq. (83) have the same order of priority. Using the constrained quadratic programming optimization algorithm of Matlab and given the cost function of Eq. (83), an improvement in the system's response can be achieved through design trade off, Mathworks et al (1998). The performance indicators and their corresponding parameters for the improved design are listed in Tables 4 and 5. These result in the following transfer function:

$$T(s) = \frac{557020}{s^3 + 58.2s^2 + 28616s + 557020} = \frac{557020}{(s+20)(s^2 + 38.2s + 27852)} \quad (84)$$

The slow pole of the system has been moved and the resulting system response is considerably faster as shown in Fig. 12.

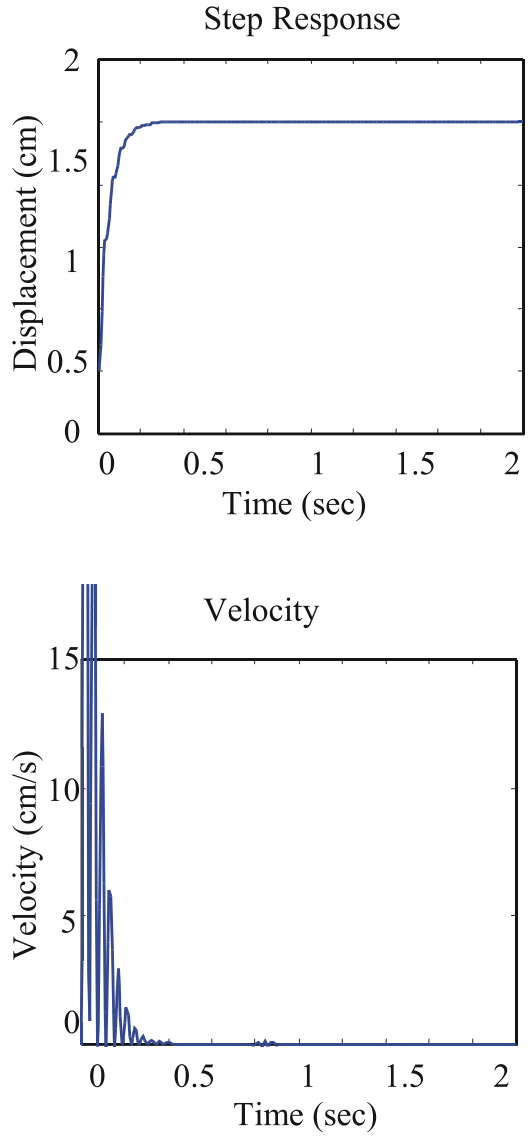

Fig. 12: *Simulated response of the improved design*

9 Conclusion

The design of a high performance hydrostatic actuation system referred to as EHA has been specified. A linearized mathematical model for this system is proposed for design analysis. A selected set of design parameters for EHA are derived from this model and are categorized as direct and indirect design parameters. This categorization is made as a measure of the parameter's accessibility to the designer.

The linearized mathematical model of EHA is used to generate functions that link the direct category of design parameters to the expected performance. These functions are used for the analysis of a prototype of EHA and for the specification of design guidelines for this class of actuation system. Experimental results from the prototype match its expected simulated performance thus supporting the validity of the model and the design guidelines. The design guidelines are used to analyze and propose an improved design for the prototype.

Nomenclature

Symbol	Definitions	Units
A	Pressure area in symmetrical actuators	[m^2]
A_{tube}	Cross-sectional area of the pipe	[m^2]
Acc	EHA positional accuracy	[m]
Acc_{DB}	Maximum accuracy not including the accuracy of the position sensor	[m]
$\bar{a}, \bar{b}, \bar{c}, \bar{d}$	Sets made up of coefficients	[-]
a_i	Characteristic polynomial coefficients	[-]
b_i, c_i, d_i	Polynomial coefficients	[-]
$DEN_T(s)$	Function	[-]
D_p	Pump volumetric displacement	[m^3/rad]
d_{sep}	Separation between the supply and actuation modules of EHA	[m]
F, F_{max}	Force	[N]
G_1, G_2, G_{CS}, T, G_{pm}	Transfer functions	[-]
I_c	Control input current	[A]
J_{pm}	Motor/pump inertia	[kgm^2]
K_{a1}	Conversion factor linking maximum actuator displacement to maximum motor speed	[rad/s/m]
K_{a2}	Conversion factor linking input to motor speed	[rad/s/V]
K_c	Motor gain	[Nm/A]
K_e	Gain of the motor's electric circuit	[A/V]
$K_{I_{cs}}$	Inner-loop integral gains	[V/rad]
K_m	Gain of the motor's mechanical part	[Nm/rad/s]

$K_{p_{CS}}$	Inner-loop proportional gain	[V/rad/s]
K_{pipe}	Pipe coefficient relating pressure drop to flow (turbulent hydraulic resistance)	[Pa/m^6/s^2]
K_{pos}	Outer-loop proportional gain	[rad/s/m]
$K_{p\,visc}$	Coefficient of viscous friction	[Nm/rad/s]
K_{ω}	Motor equivalent viscous-friction constant	[Nm/rad/s]
L	Leakage coefficient	[m^3/s/ (Nm^{-2})]
L_c	Motor line to line inductance	[H]
P_1, P_2	Actuator chamber pressures	[Pa]
P_a, P_b	Pump port pressures	[Pa]
P_{max}	Maximum system pressure	[Pa]
$P_{sensor_{acc}}$	Accuracy of the outer-loop position sensor	[m]
Q_1, Q_2	Actuator flows	[m^3/s]
Q_a, Q_b	Pump flow	[m^3/s]
Q_L	Load flow	[m^3/s]
R_c	Motor line to line resistance	[Ω]
R, I	Real and imaginary parts of a complex function	[-]
s	Laplace operator	[-]
T_{DB}	Nonlinear friction (including static and Coulomb) at the pump motor interface	[Nm]
T_m	Motor torque	[Nm]
$t_{rise}, t_{settling}$	Rise time and settling time	[s]
V_a, V_b	Pump section volumes associated with its two ports	[m^3]
V_c	Control input voltage	[V]
V_0	Total mean volume	[m^3]
$V_{0_{acc}}$	Pipe plus mean actuator chamber volume	[m^3]
$V_{residual}$	Residual volume in the actuator	[m^3]
$V_{sensor_{acc}}$	Inner-loop speed sensor accuracy	[rad/s]
x_o, x	The mean position and displacement from the mean position	[m]
X_i, Y_i	Real numbers	[-]
α, χ	Variables used for parameter plane analysis	[-]
β_e	Effective bulk modulus of hydraulic oil	[Pa]
γ	$K_{P_{CS}} / K_{I_{CS}}$	[s]
κ_h	Hydraulic subsystem gain	[m/rad/s]
$\kappa_1, \kappa_2, \kappa_3$	Polynomial coefficients	[-]
v_{max}	Maximum load velocity	[m/s]
θ	Motor angular position	[rad]
σ	Real number	[-]
τ_e	Time constant of the motor's electric circuit	[s]
τ_m	Time constant of the motor's mechanical part	[s]
τ_{pm}	Time constant	[s]
Ω_p	Accuracy of the inner-loop pump-speed controller	[rad/s]
ω	Angular frequency	[rad/s]
ω_d	Demanded pump angular velocity	[rad/s]
ω_n	Natural frequency	[rad/s]
ω_{n_h}	Hydraulic subsystem natural frequency	[rad/s]
ω_p	Pump angular velocity	[rad/s]
ξ	Pump cross-port leakage coefficient	[m^3/s/(Nm^{-2})]
ζ	Damping ratio	[-]
ζ_h	Hydraulic subsystem damping ratio	[-]

References

Anderson J., Krus, P. and Nilsson, K. 1998. *Optimization as a support for selection and design of aircraft actuation systems*. America Institute of Aeronautics and Astraunautics, AIAA-98.

Arnautovic, S. 1993. *Electrohydraulic actuator*. Technical Report, Univ. Toronto.

Del Toro, V. 1990. *Basic electric machines*. Prentice Hall.

Doeblin, E. 1972. *System dynamics modeling and response*. Charles E. Merril Publishing Co.

Habibi, S. R. and Goldenberg, A. A. 1999a. Design of a new high performance ElectroHydraulic Actuator. *IEEE/ASME International Conference on Advanced Intelligent Mechatronics, Aim'99*, Atlanta, pp. 227-232.

Habibi, S. R. and Goldenberg, A. A. 1999b. Design and analysis of a symmetrical linear actuator for hydraulic systems. *Transaction of the CSME*, Vol. 23, No. 3 & 4, pp. 377-397.

Habibi, S. R. and Goldenberg, A. A. 1999c. Design of a new high performance ElectroHydraulic Actuator. *IMECE 99, ASME*, Nashville, pp. 9-15.

Hunter, I. 1985. *Novel actuators for use in robotics and telerobotics*. Technical Report. McGill University.

Korn, J. 1972. *Hydrostatic transmission systems*. Int. Textbook Ltd.

Manring, N. D. and Luecke, G. R. 1998. Modeling and designing a hydrostatic transmission with a fixed-dis. motor, *Journal of Dyn. Sys. Meas. & Cont.* Vol 120, pp. 45-50.

Mathworks Inc. 1998. *User's manual.* Optimization Toolbox.

Merrit, H. E. 1967. *Hydraulic control Systems.* John Wiley & Sons.

Siljak, D. D. 1969. *Nonlinear systems.* John Wiley & Sons.

Vande Vegte, J. 1994. *Feedback control systems*. Prentice Hall.

Watton, J. 1989. *Fluid power systems*. Prentice Hall.

Saeid Habibi
obtained his Ph.D. in Control Engineering and Robotics from University of Cambridge, U.K. He spent a number of years in industry as a Project Manager and Senior Consultant for Cambridge Control Ltd, U.K. and as Manager of Systems Engineering for Allied Signal Aerospace Canada. He received 2 corporate recognition awards for his contributions to the Allied Signal Systems Engineering Process in 1996 and 1997. He was the recipient of the Institution of Electric Engineers (IEE) F.C. Williams best paper award in 1992. His academic background includes research into design and analysis of hydraulic actuation systems, sensors and instrumentation, and advanced multivariable control. He is on the Editorial Board of the Transactions of the Canadian Society of Mechanical Engineers and is a member of IEEE. He is currently an Associate Professor in Mechanical Engineering at the University of Saskatchewan, Canada.

Gurwinder Singh
was born in Punjab, a northwest province of India. He received the B.E. degree in mechanical engineering from Guru Nanak Dev Engineering College affiliated to "Punjab Technical University", India, in 1998. He joined the University of Saskatchewan, Saskatoon, Canada in September 1998, where he is currently pursuing the M.Sc. degree in mechanical engineering. His research interest includes closed loop control systems, multi-objective design optimization & evolutionary programming.